Journal of Colloid and Interface Science 484 (2016) 10–16

Contents lists available at ScienceDirect

Journal of Colloid and Interface Science

journal homepage: www.elsevier.com/locate/jcis

Regular Article

The effect of surfactant chain length on the morphology of poly(methyl methacrylate) microcapsules for fragrance oil encapsulation

Alison Louise Tasker [a,b,*], James Paul Hitchcock [b], Ling He [b], Elaine Alice Baxter [c], Simon Biggs [a], Olivier Jean Cayre [b]

[a] Faculty of Engineering, Architecture and Information Technology, University of Queensland, St Lucia, Queensland 4072, Australia
[b] School of Chemical and Process Engineering, University of Leeds, Woodhouse Lane, Leeds LS2 9JT, United Kingdom
[c] Procter & Gamble, London Innovation Centre, Rusham Park, Whitehall Ln, Egham TW20 9NW, United Kingdom

GRAPHICAL ABSTRACT

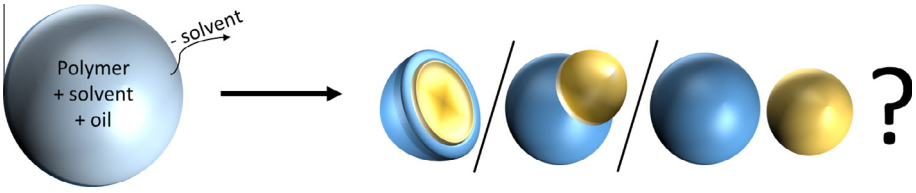

ARTICLE INFO

Article history:
Received 23 June 2016
Revised 22 August 2016
Accepted 23 August 2016
Available online 24 August 2016

Keywords:
Encapsulation
Morphology
Wetting
Polymeric microcapsules

ABSTRACT

The solvent evaporation method for producing microcapsules relies upon the correct wetting conditions between the three phases involved in the synthesis to allow core-shell morphologies to form. By measuring the interfacial tensions between the oil, polymer and aqueous phases, spreading coefficients can be calculated, allowing the capsule morphology to be predicted. In this work we explore the effect of surfactant chain length on capsule morphology using poly(methyl methacrylate) as the polymer and hexadecane as the core. We compared the predicted morphologies obtained using the polymer as a solid, and the polymer dissolved in dichloromethane to represent the point at which capsule formation begins. We found that using the polymer in its final, solid form gave predictions which were more consistent with our observations. The method was applied to successfully predict the capsule morphologies obtained when commercial fragrance oils were encapsulated.

1. Introduction

The manufacture of liquid core microcapsules is of considerable practical interest across a range of industries for the encapsulation of active ingredients including drugs [1], pesticides [2], flavours [3,4], enzymes [5] and fragrances [6]. In most cases, such microcapsules are designed to protect the actives from unfavourable external conditions and to control their subsequent release. There are various methods which can be used to create liquid core microcapsules [7]. For example interfacial polymerization can be used to create a polymer shell around an oil droplet dispersed in water (or the reverse system), by reacting monomers in the oil

Abbreviations: C_{12}TAB, dodecyltrimethylammonium bromide; C_{14}TAB, tetradecyltrimethylammonium bromide; C_{16}TAB, hexadecyltrimethylammonium bromide; C_{18}TAB, octadecyltrimethylammonium bromide; C_{10}DAB, didecyldimethylammonium bromide; C_{12}DAB, didodecyldimethylammonium bromide; CMC, critical micelle concentration; DCM, dichloromethane; PMAA, poly(methacrylic acid); PMMA, poly(methyl methacrylate); PVA, poly(vinyl alcohol); γ_{ow}, oil-water interfacial tension; γ_{pw}, polymer-water interfacial tension; γ_{op}, oil-polymer interfacial tension; S_x, spreading coefficient.

* Corresponding author at: Faculty of Engineering, Architecture and Information Technology, University of Queensland, St Lucia, Queensland 4072, Australia.
E-mail address: a.tasker@uq.edu.au (A.L. Tasker).

http://dx.doi.org/10.1016/j.jcis.2016.08.058
0021-9797/

phase with monomers in the aqueous phase [8]. Other methods lead to the production of colloidosomes [9–11], liposomes [12] and dendrimers [13], which have been used to encapsulate various active materials, such as pharmaceuticals [13–15], enzymes [12,16–19] and dyes [20–24].

Another method, which we will use in this work, involves the preparation of liquid core/polymer shell structures via a solvent extraction method, which induces a polymer to precipitate as a film (the shell) at the oil/water interface. In this method the core to be encapsulated (the encapsulate) and the polymer are initially dissolved in a highly volatile solvent and emulsified into a stabilizer solution. The volatile solvent is subsequently extracted from the emulsion droplets, resulting in the core material being encapsulated by the precipitated polymer shell [25–28]. Here, it is crucial that the solvent contained in the emulsion dispersed phase is a good, but highly volatile solvent for the polymer and that the encapsulate is a non-solvent for the polymer, so that precipitation is induced upon extraction of the solvent [26].

In this work, we initially use poly(methyl methacrylate) (PMMA) as the polymer forming the capsule shell, dichloromethane (DCM) as the good solvent, and hexadecane as the encapsulate. Subsequently, we exchange the hexadecane for various oils commonly used as fragrance oils in cosmetic and personal care products. The solution of polymer and encapsulate oil in DCM forms the core phase. The core phase is emulsified in an aqueous solution of a stabilizer, in our case a surfactant [26,29,30], but polymers [25,26,31–33] and particles [34] have also been successfully used. The resulting emulsion is diluted, allowing the DCM to evaporate slowly, creating polymer-rich droplets of DCM within the oil phase. It is believed that at this stage, the droplets are mobile and migrate to the oil-water interface, whereupon the remaining solvent leaves the core phase thus forcing the polymer to precipitate and to form a shell around the non-solvent core [25,29,35].

As depicted in Fig. 1, this process can lead to several possible morphologies in addition to the desired core-shell morphology where the polymer forms a complete shell around a single core. Alternative morphologies include acorns, where the polymer precipitates separately to the oil, occluded capsules, where the polymer precipitates around multiple cores or complete dissociation between the core and the shell.

The resulting capsule morphology is controlled by the balance of interfacial tensions for the three phases involved in the capsule formation and relates to the wetting conditions within the system. Torza and Mason studied the behaviour of systems where two immiscible liquid droplets were brought together in a third, mutually immiscible liquid [36]. By measuring the interfacial tensions between the three phases, they predicted the equilibrium morphology of the droplets from the resulting spreading coefficients. Eq. (1) shows, as an example, how the spreading coefficient is calculated.

$$S_3 = \gamma_{12} - (\gamma_{23} + \gamma_{13}) \quad (1)$$

where γ_{12} is the interfacial tension between phases 1 and 2. When phase 2 is the aqueous phase, as is usually the case [37], and phase 1 is taken to be that of highest interfacial tension with water (as compared to phase 3), it follows that there are only three possible combinations of spreading coefficients, as shown by Eqs. (2)–(4).

$$S_1 < 0,\ S_2 < 0,\ S_3 > 0 \quad (2)$$

$$S_1 < 0,\ S_2 < 0,\ S_3 < 0 \quad (3)$$

$$S_1 < 0,\ S_2 > 0,\ S_3 < 0 \quad (4)$$

For a core-shell morphology to successfully form, the polymer must be able to wet the oil in the aqueous phase preferentially (see Fig. 1). Several studies have considered the effect of these spreading coefficient combinations on capsule morphology [26,29,38–40]. Loxley and Vincent measured the interfacial tension between the oil phase and various aqueous phases using the DuNuoy ring method, and calculated the polymer-oil and polymer-aqueous phase interfacial tensions from contact angle measurements of oil and water droplets on dry films of the polymer forming the capsule shell [26]. Using this method they found that, for the range of stabilizers they tested, only the polymeric stabilizers were suitable to form core-shell morphologies. Feczkó et al. also used contact angle measurements to calculate the interfacial tension between the shell material and the other two phases and used pendant drop tensiometry to measure interfacial tensions between the liquid phases [38]. They found that this method accurately predicted the final capsule morphology obtained when using poly(methacrylic acid) (PMAA) as a stabilizer, but that the predictions failed for the other two stabilizers used, poly(vinyl alcohol) (PVA) and Tween 80. Pisani et al. also used pendant drop tensiometry to measure the interfacial tensions between the various phases [29]. However, they assumed the polymer phase would still be dissolved in the co-solvent at the time of migration to the oil-water interface, and that this was the critical point at which spreading occurs. Consequently, they measured the interfacial tension of polymer-DCM solutions rather than using a dry polymer film to perform contact angle measurements [26,38–40]. Using a selection of polymers and surfactants to stabilize their capsules, they found that Torza and Mason's spreading coefficient method did not accurately predict the final capsule morphology in two out of the three cases they investigated.

Initially in this work, we aim to ascertain whether it is possible to predict the morphology of capsules synthesized using a common cationic surfactant family, studying both the effect of the hydrocarbon chain length and the number of chains attached to the head group. We compare the ability of the prediction methods reviewed above by measuring the polymer–surfactant interfacial tension using either a dry polymer film or a polymer solution in DCM. The model systems investigated in this part of the work are based on a hexadecane core. The final objective of this work is to use the chosen prediction methodology to verify its ability to predict the morphology of structures obtained for a range of fragrance oils to

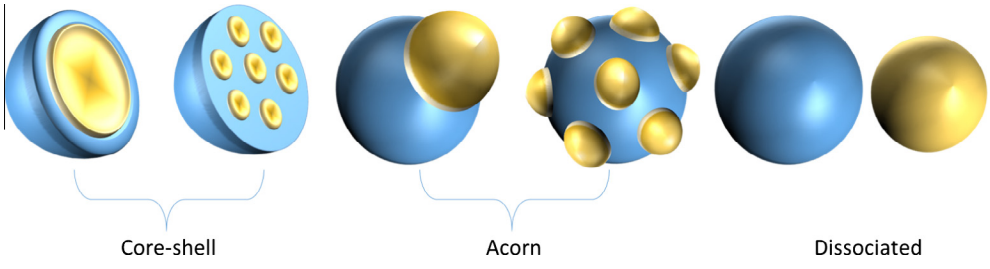

Fig. 1. Possible final microcapsule morphologies (post solvent-evaporation) dependent on spreading coefficients of the different phases. From left to right, core-shell morphologies result when Eq. (2) is satisfied, multi core-shell morphologies result when Eq. (2) is satisfied and $S_3 \gg 0$ and acorn morphologies result when Eq. (3) is satisfied, and dissociation results when Eq. (4) is satisfied.

be encapsulated by solvent-extraction, using a common surfactant from the studied series.

2. Methods

2.1. Materials

Poly(methyl methacrylate) (PMMA) (120 kDa) was purchased from Sigma-Aldrich. *N*-hexadecane, 99%, dichloromethane (DCM) >99%, and toluene, 99% were obtained from Acros Organics. Stabilizers, dodecyltrimethylammonium bromide (C_{12}TAB) >98%, tetradecyltrimethylammonium bromide (C_{14}TAB) 98%, hexadecyltrimethylammonium bromide (C_{16}TAB) 98%, octadecyltrimethylammonium bromide (C_{18}TAB) >98%, Didecyldimethylammonium bromide (C_{10}DAB) 98%, and didodecyldimethylammonium bromide (C_{12}DAB) 98% were purchased from Sigma-Aldrich. Hexyl salicylate, dihydromyrcenol and cyclamen aldehyde were provided by Procter and Gamble. All solutions were made up using ultra-pure Milli-Q water (resistivity 18 MΩ·cm).

2.2. Interfacial tension measurement

Interfacial tension measurements were carried out using the pendant drop method using a KSV CAM200 tensiometer (Biolin Scientific, Finland). PMMA (5 wt%) dissolved in DCM (method 2), and hexadecane drops were dispensed into the aqueous stabilizer solutions. For each different system, at least 10 individual drops were used to calculate the quoted mean of interfacial tensions. All experiments were conducted at 21.6 ± 0.1 °C, using droplets close to the critical detachment volume, and a horizontal needle tip, with an inner diameter 0.51 mm, to ensure accurate measurements were conducted [41].

The interfacial tension was calculated from the droplet shape recorded on the pendant drop tensiometer by fitting the Young-Laplace equation to the droplet profile:

$$\gamma = \Delta\rho g \frac{R_0^2}{\beta} \tag{5}$$

where γ is the surface or interfacial tension, $\Delta\rho$ the density difference between the drop and the surrounding medium, g the gravitational constant, R_0 the radius at the drop apex and β the shape factor.

2.3. Contact angle measurement

Contact angle measurements were used to calculate the PMMA-hexadecane interfacial tension for the case where DCM was not present in the system (method 1) as compared to method 2 where DCM is present in the system (thus the interfacial tension was measured directly).

The contact angle was measured using the sessile drop technique, using the KSV CAM200 system and software. Drops of hexadecane, or surfactant solution were deposited onto a PMMA film and the equilibrium contact angle measured for at least 5 different drops before a mean value was calculated. The PMMA film was spin-coated onto a glass slide from a 5 wt% solution of PMMA in DCM.

In cases where the contact angle between the oil or surfactant solution and polymer was too low to be measured accurately, it was taken to be <5°. Surface tension measurements of the oil or surfactant phase in air, and literature surface energy value of PMMA [42] were used to calculate the oil/water-polymer interfacial tension, using the following equation:

$$\gamma_{op} = \gamma_p + \gamma_o \cos\theta \tag{6}$$

where γ_{op} is the polymer-oil interfacial tension, γ_p is the polymer surface tension γ_o is the oil surface tension, and θ is the measured polymer-oil contact angle.

2.4. Synthesis and characterisation of polymeric capsules with oil core

Each surfactant used in the study was used at a concentration chosen to be well above the critical micelle concentration, CMC, in all cases. The concentrations were chosen to ensure that after emulsification of the oil-water systems the bulk surfactant concentration remained above the CMC, for consistency across all surfactant types used in this study. The concentrations used can be seen in the Supplementary information (Table S1). An example method is given below for C_{16}TAB.

PMMA (10 g) was dissolved in DCM (76 g). The oil to be encapsulated (14 g) was added and mixed until a single phase formed. This was used as the emulsion dispersed phase. The desired surfactant, in this case C_{16}TAB, (0.28 g) was dissolved into 100 mL Milli-Q water to form the emulsion continuous phase. The dispersed phase (7 mL) and continuous phase (7 mL) were added to a glass vial and emulsified (using IKA T25 Ultra-Turrax) at 15000 rpm for 2 min. The emulsion was then stirred magnetically at 400 rpm while a further 86 mL of continuous phase was poured in slowly. The diluted emulsion was then stirred at 400 rpm for 24 h at room temperature to allow capsule formation to occur – this stage allows for extraction of DCM into the continuous phase and subsequent evaporation, which forces precipitation of the polymer onto the emulsion droplet surface. All experiments were conducted at temperatures between 21 °C and 22 °C to attempt to minimise the effect of temperature on the resulting wetting properties of the system in comparison to the measurements of interfacial tensions made at T = 21.6 ± 0.1 °C.

The resulting capsules underwent three washing steps via centrifugation (Heraeus Megafuge R16) at 1756G for 5 min, during which the supernatant was removed and replaced with fresh Milli-Q water to remove remaining traces of DCM. Finally, the capsules were redispersed in 50 mL Milli-Q water. Colloidal stability of the prepared capsules was verified over the timescale of the procedure through light scattering measurements.

The resulting structures were studied using an Olympus BX51 optical microscope, and a LEO 1530 Gemini field emission gun scanning electron microscopy (FEGSEM).

3. Results and discussion

3.1. Comparing capsule morphology predictions

The microcapsules were formed using the solvent extraction method, a modification of that described by Loxley and Vincent [26]. The aqueous phase contained the relevant surfactant from the investigated series of single chain or double chain cationic surfactants (listed in Table 1). Each surfactant was used in a concentration which was well in excess of the CMC, before and after saturation at the total emulsion interface. As a result, the conditions under which spreading of the precipitating polymer films occurred were as close as possible for each experiment. A table (S1) of CMC, the molar concentration used in the aqueous phase before emulsification and the calculated final bulk concentration after emulsion production for each surfactant can be found in the Supplementary information. For each experiment the core phase was emulsified with an aqueous solution of the surfactant in a 1:1 ratio of core to aqueous phase. Once formed, the emulsion was diluted with the same surfactant solution (same concentration) to allow for controlled extraction of DCM from the oil

Table 1
Measured interfacial tensions, calculated spreading coefficients of the different phases involved in the microcapsule formation process and morphology predictions and observations of PMMA-hexadecane microcapsules for different stabilizers. Calculations here are made using interfacial tension measurements carried out with dry **PMMA films** (method 1).

Stabilizer	γ_{ow}/mN·m^{-1}	γ_{pw}/mN·m^{-1}	γ_{op}/mN·m^{-1}	S_1	S_2	S_3	Predicted	Observed
C_{12}TAB	10.1(±0.1)	20.5(±0.3)	14.2(±0.6)	−24.6	−16.4	−3.8	Acorn	Acorn
C_{14}TAB	5.4 (±0.1)	18.5(±0.5)	14.2(±0.6)	−27.3	−9.7	−1.1	Acorn	Acorn
C_{16}TAB	4.7(±0.1)	18.2(±0.1)	14.2(±0.6)	−27.7	−8.7	−0.7	Acorn	Acorn
C_{18}TAB	3.7(±0.6)	17(±2)	14.2(±0.6)	−27.5	−6.5	−0.9	Acorn	Acorn
C_{10}DAB	⩽1	15.7(±0.2)	14.2(±0.6)	⩽−29	⩽−1	⩾1	Core-shell	Core-shell
C_{12}DAB	⩽1	16.5(±0.3)	14.2(±0.6)	⩽−30	⩽−2	⩾1	Core-shell	Core-shell

dispersed phase into the aqueous phase. The loss of DCM drastically reduces the polymer solubility in the core phase, which induces precipitation on the surface of the oil droplets. The resulting structures were analysed via light and electron microscopy and the observed shapes were compared with predictions made on the basis of interfacial tension measurements between the three phases involved.

Interfacial tensions between all three phases involved were measured for all stabilizers discussed above, and the data were used to calculate the spreading coefficients of each of the phases using Eq. (1). Interfacial tensions and resulting spreading coefficients data are presented in Table 1. The combination of the spreading coefficients for each system allows the prediction of the resulting capsule morphology as demonstrated with Eqs. (2)–(4). The values for the interfacial tensions are obtained using two different methods. In the first method, the interfacial tension between polymer and water ($\boldsymbol{\gamma_{pw}}$) is obtained using a dry PMMA film for the measurements. In the second method however, the same interfacial tension $\boldsymbol{\gamma_{pw}}$ is obtained using a polymer phase containing DCM and thus in a liquid state.

When using the first method, for all of the single chain surfactants used in this study (C_xTAB) the predicted morphology is acorn, whereas for each of the double chain surfactants (C_xDAB) a core-shell morphology is predicted (Table 1). The measurements for the polymer-water interfacial tensions appear to be higher for the shortest hydrocarbon tails, which denotes a more efficient wetting of the polymer films for the longer chain surfactants. The oil–aqueous phase interfacial tension, whilst very low in all cases, also appears to become smaller with increasing surfactant chain length. This is likely due to improved packing of the hydrocarbon tail at the liquid-liquid interface as the chain length increases, while the area occupied by the surfactant head does not vary. When considering the double chain surfactants, the interfacial tensions recorded are too low for a consistent trend to be observed for the influence of chain length for the studied surfactants. It is worth noting that due to the error associated with the interfacial tension measurements, the spreading coefficients calculated have an inherent error themselves. Therefore when the spreading coefficient is close to zero, the uncertainty in the interfacial tension measurements can potentially lead to inaccurate predictions. In Table 1 however, whilst all of the S3 values are close to zero, the predictions do in fact match the capsule morphologies observed experimentally.

Work in the literature has developed an alternative method for predicting the final capsule morphology [29]. Indeed, Pisani et al. suggest that the critical step of capsule formation, responsible for the final morphology, is the onset of polymer precipitation. At this point DCM is still present in the core and the polymer is dissolved in pockets of DCM, which migrate to the surface of the oil droplet. To replicate this specific part of the process, these authors measured the interfacial tensions involving the polymer phase when the latter was dissolved in the good solvent. Here we replicated these measurements for our system using the second method for interfacial tension measurements described above. Thus interfacial tensions were measured for the polymer dissolved in DCM for a selection of surfactants from the previous study.

Table 2 shows the predicted capsule morphologies using the method suggested by Pisani et al. [29] For the polymer-water interfacial tension, the values in all cases are much lower than those seen when the polymer phase is used as a solid. The spreading coefficient, S_2, in the case of C_{12}TAB, is zero which results in an ambiguous prediction of either acorn or dissociated structures. Using this method the prediction from C_{18}TAB also does not reflect the observed morphology. Thus, for the cases studied here, the presence of DCM when measuring the interfacial tension between the polymer phase and the aqueous phase appears to lead to less accurate predictions. By using the PMMA-DCM solution for the measurements needed to calculate spreading coefficients, the interfacial tension between polymer and oil phase could not be directly measured as hexadecane dissolves in DCM. Thus the value for the hexadecane-PMMA interfacial tension was calculated from the contact angle of hexadecane on a dry PMMA film, using the literature surface tension measurement of PMMA [42] as in the previous part of the work. This is a limitation of this method, which potentially contributes to the inaccuracy of the predictions in this case.

Fig. 2 presents electron micrographs illustrating the observed capsule morphologies obtained when each of the different surfactants are used. Fig. 2a shows that when choosing C_{12}TAB as the stabilizer acorn, morphologies are predominantly formed as predicted. However, as suggested by the predictions in Table 2, some dissociated structures are visible. An example of such structure is given (Fig. S1) in the Supplementary information. In Fig. 2b, when C_{14}TAB is used as the stabilizer, the morphology obtained is acorn. This is predicted from the three negative spreading coefficients calculated from the measured interfacial tensions. By applying mechanical force to the samples before observations using optical microscopy, no oil can be observed upon deformation of the polymer structures confirming that these do not contain any encapsulated core.

It is clear from the scanning electron micrographs displayed in Fig. 2c that C_{16}TAB stabilised capsules do not form a core-shell morphology. The majority of the capsules show an acorn structure, with some of the larger capsules resulting in multiple pores or dents on their surface, where smaller oil droplets have de-wetted from the polymer surface [26]. The morphologies seen in Fig. 2c are supported by Loxley and Vincent's findings that C_{16}TAB stabilised PMMA capsules with a hexadecane core do not form core-shell morphologies [26].

Acorn morphologies are also obtained (Fig. 2e) when C_{18}TAB is used as the emulsion stabilizer. This is due to a further decrease of the interfacial tension between oil and water (as compared to smaller chain surfactants in this series) as also confirmed by the predictions in Table 1.

Fig. 2e and f presents scanning electron micrographs of the resulting capsule morphology when double chained surfactants,

Table 2
Measured interfacial tensions, calculated spreading coefficients of the different phases involved in the microcapsule formation process and morphology predictions and observations of PMMA-hexadecane microcapsules for different stabilizers. Calculations here are made using interfacial tension measurements involving the polymer phase carried out with **PMMA dissolved in DCM** (method 2).

Stabilizer	γ_{ow}/mN·m^{-1}	γ_{pw}/mN·m^{-1}	γ_{op}/mN·m^{-1}	S_1	S_2	S_3	Predicted	Observed
C_{12}TAB	10.1(±0.1)	4.1(±0.3)	14.2(±0.6)	−20.2	0	−8.2	Acorn/dissociated	Acorn
C_{16}TAB	4.7(±0.1)	5.2(±0.2)	14.2(±0.6)	−14.6	−4.3	−13.8	Acorn	Acorn
C_{18}TAB	3.7(±0.6)	9.4(±0.7)	14.2(±0.6)	−19.9	1.1	−8.6	Dissociated	Acorn
C_{10}DAB	⩽1.0	16.0(±2.0)	14.2(±0.6)	⩽−29	⩽−1	⩾1	Core-shell	Core-shell

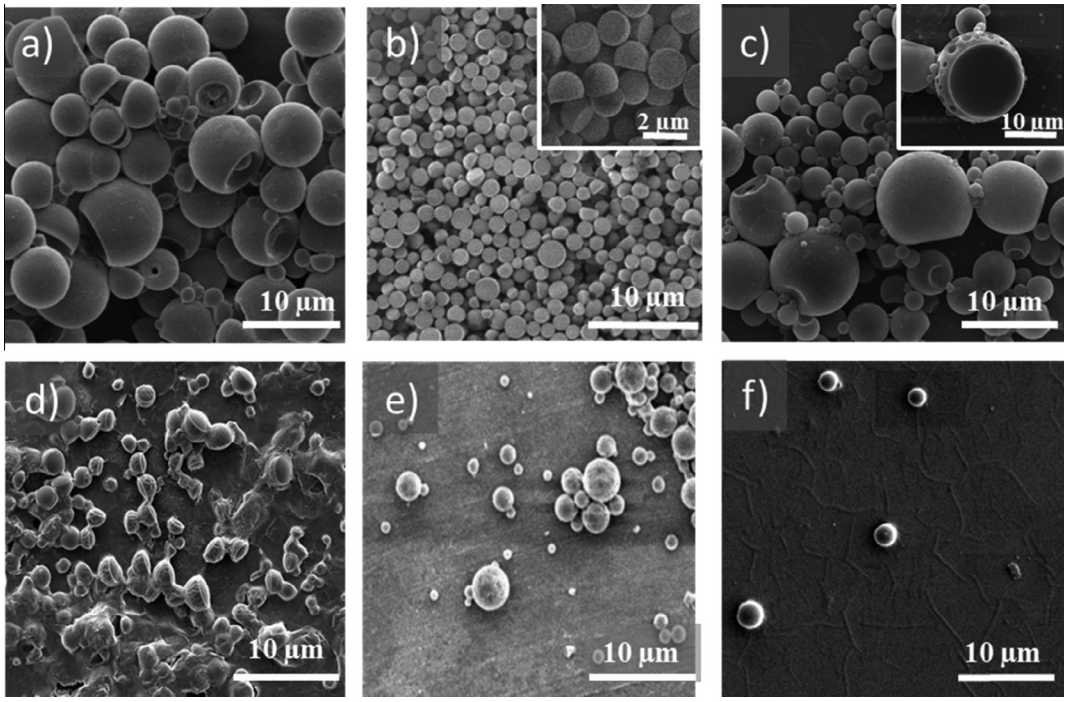

Fig. 2. Scanning electron micrographs showing acorn morphologies when the stabilizer used is C_{12}TAB (a), C_{14}TAB (b), C_{16}TAB (c) or C_{18}TAB (d). The inset in (c) illustrates observations made of larger multi-acorn morphologies for the C_{16}TAB surfactant. (e) and (f) show core-shell morphologies obtained when using C_{10}DAB and C_{12}DAB as the stabilizer, respectively.

C_{10}DAB and C_{12}DAB respectively, are used as the stabilizer. As predicted from the spreading coefficients, in each case a core-shell morphology is produced. This is confirmed when mechanically rupturing the capsule shell between two glass slides, which shows broken capsules and evidence of leaching oil when observed via optical microscopy. Although for each of the twin tailed surfactants used in this study the desired core-shell morphology is observed, the capsule yield is much lower than that when a single chain cationic surfactant is used. This could be due to the poor solubility of these surfactants at room temperature, which have a tendency to form micellar or laminar phases. Indeed excess polymer is seen to precipitate into the bulk during capsule formation, suggesting there is not enough surfactant available to adsorb at the oil-water interface. In addition, the poor water solubility of these surfactants, could allow partitioning into the oil phase, which may decrease the oil-polymer interfacial tension thus promoting core-shell capsule morphology formation. Despite the fact that both methods correctly predict the morphology for these surfactants, it is possible that partition of these surfactants into the oil phase influences the accuracy of the interfacial tension measurements (with respect to what occurs in the capsule formation process). Double chain cationic surfactants such as the ones used here have a packing parameter of around 0.6, as compared to the single chain surfactants which typically have a packing parameter of around 0.3 [43]. This means that the double chain surfactants have a tendency to form w/o emulsions, rather than the o/w emulsions the microcapsule preparation method relies upon. However, Evans et al. showed that upon dilution of a w/o emulsion stabilised with C_{12}DAB, spontaneous inversion of the emulsion occurred to form an oil-in-water emulsion of uniform size distribution [44,45]. In our case, for both double chain surfactants, fluorescence microscopy images (Fig. S2) confirm that a w/o emulsion is formed prior to dilution, while the emulsion appears to phase invert to an o/w emulsion upon dilution. This phase inversion, coupled with the slower rearrangement of double chained surfactants at the interface, as evidenced by their lower diffusion coefficient (10^{-7} cm^2·s^{-1}) [46] as compared with the single chained counterpart (10^{-6} cm^2·s^{-1}) [47], could be the cause of the lower capsule yield obtained in this study. This phase inversion of the emulsion after dilution is common to the double chain surfactants investigated here. Whilst they form the desired core-shell capsules, it is important to note that the mechanism of capsule formation is different to that of the single chain surfactants and so cannot be directly compared. To prevent this mechanism from driving the capsule formation, the emulsions stabilised with the double-chained surfactants were formed with a water:oil ratio of 9:1, resulting in the direct formation of an o/w emulsion prior to dilution with additional Milli-Q water (see Fig. S2).

The work above thus allows us to compare the two different methods for measuring the interfacial tensions of the three phases

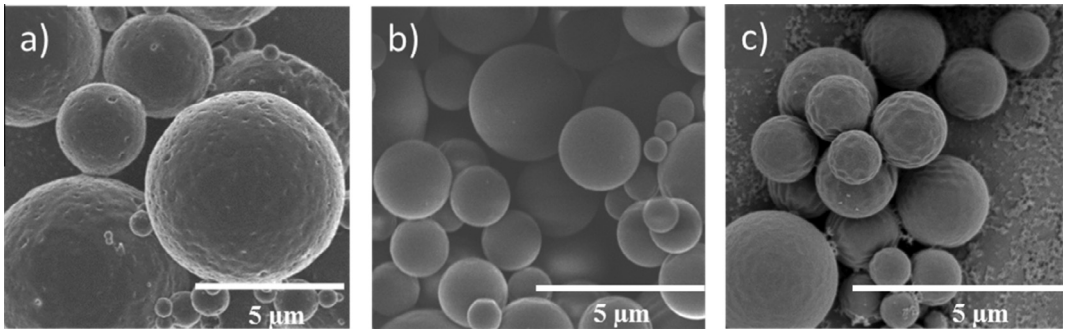

Fig. 3. Scanning Electron Micrographs of core-shell morphologies when (a) hexyl salicylate, (b) cyclamen aldehyde and (c) toluene are used as the core oil.

involved in the preparation of the microcapsules and the corresponding predictions through calculation of the spreading coefficients. For this surfactant series, it is clear that measuring the interfacial tensions of the final capsule components with the solid PMMA film rather than the PMMA-DCM solution is more efficient.

3.2. Encapsulating fragrance oils using C_{16}TAB stabilised microcapsules

In the first part of this work, we have used hexadecane as our model encapsulate oil. This allowed us to develop a robust method of predicting the final capsule morphology of PMMA capsules as a function of the choice of surfactant used as the stabilizer. Additionally, this oil phase also allows comparison of the data with that of previous work by Loxley and Vincent [26]. Based on the results from the previous section, interfacial tensions between the three phases of the final capsule components (method 1) are used here to predict the capsule morphology obtained when encapsulating a range of more polar, commercial fragrance oils. We found that the use of double-chain surfactants induces similar challenges with these oils, forming a w/o emulsion initially and thus giving a very low yield ultimately. Therefore single chain surfactants would be preferred. By measuring the interfacial tensions of the systems using C_{16}TAB, the most commonly used surfactant, all oils were predicted to be appropriately encapsulated in core-shell structures, and therefore we chose this specific surfactant and confirmed successful encapsulation. Hexyl salicylate, dihydromyrcenol and cyclamen aldehyde were chosen, as good examples of fragrance oils used in perfumes and other personal care products.

From the data shown in Table 3, it is clear that all the predicted and observed capsule morphologies agree, and a successful encapsulation of every fragrance oil tested in this part of the study was achieved. It is worth noting that in the case of toluene, the spreading coefficient S3 is close to 0 but positive, which warrants prediction of a core-shell structure albeit with some doubts over the accuracy. While this needs to be taken into account, when considering the validity of the predictions, all morphologies obtained with the different oils are correctly predicted as core-shell structures (see Fig. 3).

4. Conclusions

In this work we have successfully predicted the resulting microcapsule morphology for PMMA capsules prepared by polymer precipitation with different stabilizers from a cationic surfactant family including single and double chain surfactants. We have used the spreading coefficients calculated from both the interfacial tensions of the three phases present in the final capsule, hexadecane core oil, solid PMMA, and surfactant solution, and the interfacial tensions for the three phases when the polymer is dissolved in DCM, to represent the point at which capsule formation begins, to predict the ultimate capsule morphology. In the case of our examples, we confirm that the most accurate predictions are found when the polymer is used as a dry film for the interfacial tension measurements [26], as opposed to when it is dissolved in the solvent used in the capsule synthesis [29]. We investigated both chain length of the surfactant hydrocarbon tails and the number of long chains on the surfactant, variables previously unreported in the literature. We found that all the single chain surfactants used in this study yield predominantly acorn structures when hexadecane is used as the core oil, whereas the double chained surfactants give core-shell capsules albeit at lower yields. The double-chained surfactants were inadequate to stabilise more polar oils such as the fragrance oils used in this study, due to their tendency to form w/o emulsions initially which leads to low yields. Therefore, predictions were made using the interfacial tensions of the final capsule components for C_{16}TAB, which successfully stabilised core-shell capsules for all cases, as suggested by the predictions. This powerful predictive tool can thus be utilised in future to confirm the resulting capsule structure for any previously unknown polymer – oil - surfactant combinations, eliminating the requirement for timely trial and error experiments.

Acknowledgements

The authors acknowledge the EPSRC for grant numbers EP/J500458/1 and EP/K503836/1, providing us with the funding to complete this work. We also acknowledge the funding received from Procter and Gamble. The authors also acknowledge the facilities, and the scientific and technical assistance, of the Australian

Table 3
The interfacial tensions, spreading coefficients and morphology predictions and observations of PMMA microcapsules stabilised by C_{16}TAB with different oil cores. Method 1 is used to measure interfacial tensions using a dry **PMMA film** for the measurements involving the polymer phase.

Oil	γ_{ow}/mN·m^{-1}	γ_{pw}/mN·m^{-1}	γ_{op}/mN·m^{-1}	S_1	S_2	S_3	Predicted	Observed
Toluene	3.3(±0.7)	18.2(±0.1)	14.3(±0.4)	−29.2	−7.2	0.6	Core-shell	Core-shell
Hexyl salicylate	3.3(±0.3)	18.2(±0.1)	<1	⩽−16	⩽−21	⩾13	Core-shell	Core-shell
Cyclamen aldehyde	1.8(±0.2)	18.2(±0.1)	11.5(±0.5)	−27.9	−8.5	4.9	Core-shell	Core-shell
Dihydro-myrcenol	2.7(±0.1)	18.2(±0.1)	14 (±0.3)	−29.3	−7.1	1.7	Core-shell	Core-shell

Microscopy & Microanalysis Research Facility at the Centre for Microscopy and Microanalysis, The University of Queensland, and the Leeds Electron Microscopy and Spectroscopy Centre.

Appendix A. Supplementary material

Supplementary data associated with this article can be found, in the online version, at http://dx.doi.org/10.1016/j.jcis.2016.08.058.

References

[1] S. Giovagnoli, F. Palazzo, A. Di Michele, A. Schoubben, P. Blasi, M. Ricci, The influence of feedstock and process variables on the encapsulation of drug suspensions by spray-drying in fast drying regime: the case of novel antitubercular drug-palladium complex containing polymeric microparticles, J. Pharm. Sci. 103 (4) (2014) 1255–1268.
[2] C. Sun, K. Shu, W. Wang, Z. Ye, T. Liu, Y. Gao, H. Zheng, G. He, Y. Yin, Encapsulation and controlled release of hydrophilic pesticide in shell cross-linked nanocapsules containing aqueous core, Int. J. Pharm. 463 (1) (2014) 108–114.
[3] Z. Yang, Z. Peng, J. Li, S. Li, L. Kong, P. Li, Q. Wang, Development and evaluation of novel flavour microcapsules containing vanilla oil using complex coacervation approach, Food Chem. 145 (2014) 272–277.
[4] M. Maswal, A.A. Dar, Formulation challenges in encapsulation and delivery of citral for improved food quality, Food Hydrocolloids 37 (2014) 182–195.
[5] F. Caruso, D. Trau, H. Mohwald, R. Renneberg, Enzyme encapsulation in layer-by-layer engineered polymer multilayer capsules, Langmuir 16 (4) (2000) 1485–1488.
[6] Y. Li, Y.-Q. Huang, H.-F. Fan, Q. Xia, Heat-resistant sustained-release fragrance microcapsules, J. Appl. Polym. Sci. 131 (7) (2014).
[7] H.N. Yow, A.F. Routh, Formation of liquid core-polymer shell microcapsules, Soft Matter 2 (11) (2006) 940–949.
[8] J. Cui, Y. Wang, A. Postma, J. Hao, L. Hosta-Rigau, F. Caruso, Monodisperse polymer capsules: tailoring size, shell thickness, and hydrophobic cargo loading via emulsion templating, Adv. Funct. Mater. 20 (10) (2010) 1625–1631.
[9] G. Liu, S. Liu, X. Dong, F. Yang, D. Sun, Rearrangement of layered double hydroxide nanoplatelets during hollow colloidosome preparation, J. Colloid Interface Sci. 345 (2) (2010) 302–306.
[10] O.J. Cayre, P.F. Noble, V.N. Paunov, Fabrication of novel colloidosome microcapsules with gelled aqueous cores, J. Mater. Chem. 14 (22) (2004) 3351–3355.
[11] D. Lee, D.A. Weitz, Double emulsion-templated nanoparticle colloidosomes with selective permeability, Adv. Mater. 20 (18) (2008) 3498–3503.
[12] S.Y. Hwang, H.K. Kim, J. Choo, G.H. Seong, T.B.D. Hien, E.K. Lee, Effects of operating parameters on the efficiency of liposomal encapsulation of enzymes, Colloids Surf. B – Biointerfaces 94 (2012) 296–303.
[13] L. Tu Uyen, T. Ngoc Quyen, H. Thi Kim Dung, P. Kim Ngoc, T. Hai Nhung, N. Cuu Khoa, Pegylated dendrimer and its effect in fluorouracil loading and release for enhancing antitumor activity, J. Biomed. Nanotechnol. 9 (2) (2013) 213–220.
[14] Y. Zhang, H.F. Chan, K.W. Leong, Advanced materials and processing for drug delivery: the past and the future, Adv. Drug Deliv. Rev. 65 (1) (2013) 104–120.
[15] T.M. Allen, P.R. Cullis, Liposomal drug delivery systems: from concept to clinical applications, Adv. Drug Deliv. Rev. 65 (1) (2013) 36–48.
[16] P.H. Keen, N.K. Slater, A.F. Routh, Encapsulation of amylase in colloidosomes, Langmuir 30 (8) (2014) 1939–1948.
[17] Z. Wang, M.C.M. van Oers, F.P.J.T. Rutjes, J.C.M. van Hest, Polymersome colloidosomes for enzyme catalysis in a biphasic system, Angew. Chem. Int. Ed. 51 (43) (2012) 10746–10750.
[18] M. Yoshimoto, Stabilization of enzymes through encapsulation in liposomes, Methods Mol. Biol. (Clifton, N.J.) 679 (2011) 9–18.
[19] B. Chaize, J.P. Colletier, M. Winterhalter, D. Fournier, Encapsulation of enzymes in liposomes: high encapsulation efficiency and control of substrate permeability, Artif. Cells Blood Substit. Immobil. Biotechnol. 32 (1) (2004) 67–75.
[20] P.J. Dowding, R. Atkin, B. Vincent, P. Bouillot, Oil core/polymer shell microcapsules by internal phase separation from emulsion droplets. Ii: Controlling the release profile of active molecules, Langmuir 21 (12) (2005) 5278–5284.
[21] C. Huo, M. Li, X. Huang, H. Yang, S. Mann, Membrane engineering of colloidosome microcompartments using partially hydrophobic mesoporous silica nanoparticles, Langmuir 30 (50) (2014) 15047–15052.
[22] Y. Gong, A.M. Zhu, Q.G. Zhang, Q.L. Liu, Colloidosomes from poly(N-vinyl-2-pyrrolidone)-coated poly(N-isopropylacrylamide-co-acrylic acid) microgels via UV crosslinking, RSC Adv. 4 (19) (2014) 9445–9450.
[23] S. Li, B.A. Moosa, J.G. Croissant, N.M. Khashab, Electrostatic assembly/disassembly of nanoscaled colloidosomes for light-triggered cargo release, Angew. Chem. Int. Ed. 54 (23) (2015) 6804–6808.
[24] R.M. Hoffman, Topical liposome targeting of dyes, melanins, genes, and proteins selectively to hair follicles, J. Drug Target. 5 (2) (1998) 67–74.
[25] T. Feczkó, J. Tóth, J. Gyenis, Comparison of the preparation of PLGA-BSA nano- and microparticles by PVA, poloxamer and PVP, Colloids Surf., A 319 (1–3) (2008) 188–195.
[26] A. Loxley, B. Vincent, Preparation of poly(methylmethacrylate) microcapsules with liquid cores, J. Colloid Interface Sci. 208 (1) (1998) 49–62.
[27] M. Dittrich, J. Hampl, F. Soukup, Branched oligoester microspheres fabricated by a rapid emulsion solvent extraction method, J. Microencapsul. 17 (5) (2000) 587–598.
[28] Z.P. Zhang, S.S. Feng, The drug encapsulation efficiency, in vitro drug release, cellular uptake and cytotoxicity of paclitaxel-loaded poly(lactide)-tocopheryl polyethylene glycol succinate nanoparticles, Biomaterials 27 (21) (2006) 4025–4033.
[29] E. Pisani, E. Fattal, J. Paris, C. Ringard, V. Rosilio, N. Tsapis, Surfactant dependent morphology of polymeric capsules of perfluorooctyl bromide: influence of polymer adsorption at the dichloromethane-water interface, J. Colloid Interface Sci. 326 (1) (2008) 66–71.
[30] J.P. Hitchcock, A.L. Tasker, E.A. Baxter, S. Biggs, O.J. Cayre, Long-term retention of small, volatile molecular species within metallic microcapsules, Acs Appl. Mater. Interfaces 7 (27) (2015) 14808–14815.
[31] F. Ito, H. Kawakami, Facile technique for the preparation of monodispersed biodegradable polymer nanospheres using a solvent evaporation method, Colloids Surf. A – Physicochem. Eng. Aspects 482 (2015) 734–739.
[32] Y. Wei, Y. Wang, L. Wang, D. Hao, G. Ma, Fabrication strategy for amphiphilic microcapsules with narrow size distribution by premix membrane emulsification, Colloids Surf. B – Biointerfaces 87 (2) (2011) 399–408.
[33] K.B. Ferenz, I.N. Waack, C. Mayer, H. de Groot, M. Kirsch, Long-circulating poly (ethylene glycol)-coated poly(lactid-co-glycolid) microcapsules as potential carriers for intravenously administered drugs, J. Microencapsul. 30 (7) (2013) 632–642.
[34] O.J. Cayre, S. Biggs, Hollow microspheres with binary porous membranes from solid-stabilised emulsion templates, J. Mater. Chem. 19 (18) (2009) 2724–2728.
[35] N.A. Wagdare, A.T.M. Marcelis, R.M. Boom, C.J.M. van Rijn, Microcapsules with a pH responsive polymer: influence of the encapsulated oil on the capsule morphology, Colloids Surf. B – Biointerfaces 88 (1) (2011) 175–180.
[36] S. Torza, S.G. Mason, 3-Phase interactions in shear and electrical fields, J. Colloid Interface Sci. 33 (1) (1970). 67-&.
[37] J. Bergek, M.A. Trojer, A. Mok, L. Nordstierna, Controlled release of microencapsulated 2-N-octyl-4-isothiazolin-3-one from coatings: effect of microscopic and macroscopic pores, Colloids Surf., A 458 (2014) 155–167.
[38] T. Feczkó, A. Kardos, B. Németh, L. Trif, J. Gyenis, Microencapsulation of N-hexadecane phase change material by ethyl cellulose polymer, Polym. Bull. 71 (12) (2014) 3289–3304.
[39] M. Andersson Trojer, A. Mohamed, J. Eastoe, A highly hydrophobic anionic surfactant at oil-water, water-polymer and oil-polymer interfaces: implications for spreading coefficients, polymer interactions and microencapsulation via internal phase separation, Colloids Surf., A 436 (2013) 1048–1059.
[40] T. Trongsatitkul, B.M. Budhlall, Multicore-shell pnipam-co-pegma microcapsules for cell encapsulation, Langmuir 27 (22) (2011) 13468–13480.
[41] J.D. Berry, M.J. Neeson, R.R. Dagastine, D.Y. Chan, R.F. Tabor, Measurement of surface and interfacial tension using pendant drop tensiometry, J. Colloid Interface Sci. 454 (2015) 226–237.
[42] P.F. Rios, H. Dodiuk, S. Kenig, S. McCarthy, A. Dotan, The effect of polymer surface on the wetting and adhesion of liquid systems, J. Adhes. Sci. Technol. 21 (3–4) (2007) 227–241.
[43] G.G. Warr, R. Sen, D.F. Evans, J.E. Trend, Microemulsion formation and phase behavior of dialkydimethylammonium bromide surfactants, J. Phys. Chem. 92 (3) (1988) 774–783.
[44] S.J. Chen, D.F. Evans, B.W. Ninham, D.J. Mitchell, F.D. Blum, S. Pickup, Curvature as a determinant of microstructure and microemulsions, J. Phys. Chem. 90 (5) (1986) 842–847.
[45] R.W. Greiner, D.F. Evans, Spontaneous formation of a water-continuous emulsion from a W/O microemulsion, Langmuir 6 (12) (1990) 1793–1796.
[46] E.F. Marques, O. Regev, A. Khan, M. da Graça Miguel, B. Lindman, Vesicle formation and general phase behavior in the catanionic mixture SDS–DDAB–water. The cationic-rich side, J. Phys. Chem. B 103 (39) (1999) 8353–8363.
[47] S.J. Candau, E. Hirsch, R. Zana, New aspects of the behaviour of alkyltrimethylammonium bromide micelles: light scattering and viscosimetric studies, J. Phys. France 45 (7) (1984) 1263–1270.